# Carrier Multiplication in a Single Semiconductor Nanocrystal

Fengrui Hu,[1] Bihu Lv,[1] Chunyang Yin,[1] Chunfeng Zhang,[1] Xiaoyong Wang,[1,*] Brahim Lounis,[2,†] and Min Xiao[1,3,‡]
[1]National Laboratory of Solid State Microstructures, School of Physics, and Collaborative Innovation Center of Advanced Microstructures, Nanjing University, Nanjing 210093, China
[2]Laboratoire Photonique Numérique et Nanosciences, Université de Bordeaux, Institut d'Optique Graduate School and CNRS, Talence 33405, France
[3]Department of Physics, University of Arkansas, Fayetteville, Arkansas 72701, USA
(Received 11 December 2015; published 9 March 2016)

To confirm the existence of the carrier multiplication (CM) effect and estimate its generation efficiency of multiple excitons in semiconductor nanocrystals (NCs), it is imperative to completely exclude the false contribution of charged excitons from the measured CM signal. Here we place single CdSe NCs above an aluminum film and successfully resolve their UV-excited photoluminescence (PL) time trajectories where the true and false CM signals are contained in the blinking "on" and "off" levels, respectively. By analyzing the PL dynamics of the on-level photons, an average CM efficiency of ~20.2% can be reliably estimated when the UV photon energy is ~2.46 times the NC energy gap.

DOI: 10.1103/PhysRevLett.116.106404

When two or more excitons are present simultaneously within a single semiconductor nanocrystal (NC), a multiexciton state is formed that plays important roles in a variety of optoelectronic devices ranging from lasers [1], photodetectors [2], solar cells [3,4], light-emitting diodes [5], and photon-pair sources [6]. In the simplest form of a multiexciton state, the two excitons can be created inside a single NC after the absorption of two low-energy photons and the subsequent cooling of the two intermediate-state electrons to the band-edge state [Fig. 1(a)]. Alternatively, the two excitons can be generated through a carrier multiplication (CM) process with the absorption of a single photon whose energy is at least twice of the NC energy gap ($E_g$). The high-state electron could relax directly to the band-edge state with its released energy pumping another valence electron to the conduction band [Fig. 1(b)]. Once a two-exciton configuration is achieved [Fig. 1(c)], it is a dominant occurrence for the biexciton recombination energy to be transferred to the single exciton instead of being converted to a photon due to the nonradiative Auger recombination effect [7]. So far, the CM effect has been not only fundamentally demonstrated in a wide range of semiconductor NCs with different compositions [8–10], but also practically utilized in several optoelectronic devices to yield improved light-to-electric conversion efficiencies [2–4]. However, it is still highly debated whether the CM efficiency is truly enhanced in semiconductor NCs due to the additional presence of charged excitons along with the neutral multiexcitons in the routine CM measurements [11–18].

There are two possible mechanisms to enhance the charging probability of a single NC in the CM process. First, as shown in Fig. 1(d) still for a two-exciton configuration, one of the charge carriers (e.g., the electron) in the single exciton can be ejected out of the NC after receiving the biexciton recombination energy [19–21]. This is in contrast to the scenario shown in Fig. 1(c) where the charge carriers of the single exciton could relax back to and recombine radiatively in the band-edge states after dissipating the biexciton recombination energy as heat.

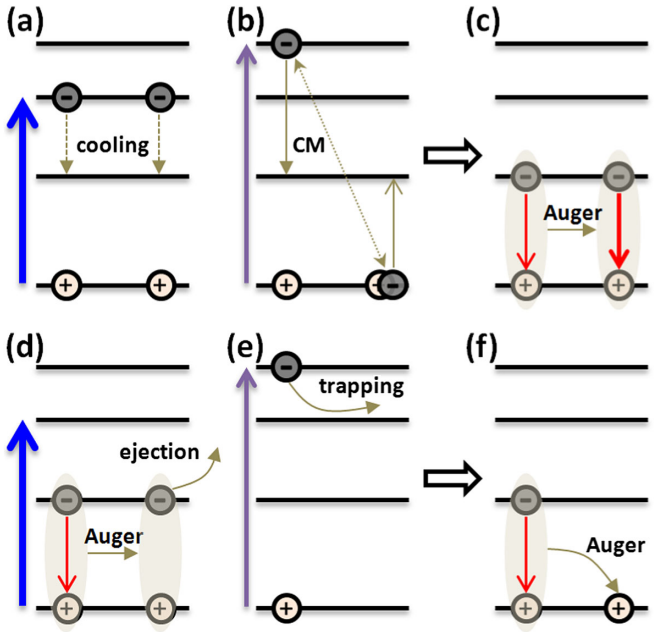


FIG. 1. (a) Two excitons can be created in a single NC after simultaneous absorption of two low-energy photons. (b) Two excitons can also be created in a single NC through the CM effect after the absorption of a single high-energy photon. (c) The single NC is left with a neutral exciton after the two-exciton Auger interaction process. (d) An extra hole is left in the single NC after the biexciton ionization process. (e) An extra hole is left in the single NC after the hot-electron trapping process. (f) Auger interaction between a single exciton and an extra hole.

 

Second, as shown in Fig. 1(e) for a high-state electron, it is more likely to be captured by external traps than would it relax from the intermediate state or stay in the band-edge state [22–24]. After either of the above two processes, the NC is left with an unpaired hole, which could couple with the electron-hole pair generated next to form a positively charged single-exciton state [Fig. 1(f)]. In this case, the single exciton is hardly emissive since its recombination energy would be mainly transferred to the extra hole also in a nonradiative Auger process [25,26]. For regular semiconductor NCs, the Auger lifetimes of the charged exciton and the neutral biexciton are both at the subnanosecond time scale [27,28], which is significantly shorter than the radiative lifetime of tens of nanoseconds for the single neutral exciton [29]. In the routine CM measurements of ensemble NCs with an ultrafast technique such as transient absorption, the existence of charged excitons would cause a delayed absorption of the probe laser beam, which can be wrongly taken as arising from CM-induced biexcitons.

In practice, the sample solution could be rigorously stirred to remove charged NCs from the probed volume of an ultrafast optical measurement and thus, the ensemble CM efficiency can be reliably estimated based on the assumption that the solution refreshing rate is faster than that of the NC charging process [12,22,30,31]. An alternative solution to the above charged-exciton issue, especially at the solid phase that is more pertaining to device applications, is to perform the CM measurements on the single NCs so that the dynamic signatures of multiexcitons and charged excitons can be extracted separately from the "on" and "off" levels of the photoluminescence (PL) blinking time trajectory. However, mainly due to the unavoidable existence of strong background fluorescence, the UV-excited PL is difficult to be detected from any single optical emitters. Here we show that the UV-excited background fluorescence can be greatly suppressed by placing polymer-wrapped single CdSe/ZnS NCs on top of an aluminum film. This has allowed us to realize the first CM measurement of a single NC at the laser wavelength of 266 nm ($\sim 2.46\, E_g$). An average CM efficiency of ~20.2% can be reliably estimated from the on-level PL decay curves of a statistically large number of single NCs.

The experimental setup for the CM measurement is schematically shown in Fig. 2(a) (see Supplemental Material [32] for experimental details), where single rod-shaped CdSe/ZnS NCs with an aspect ratio of ~1.8 (Ref. [33]) and an emission peak of 655 nm (see Fig. S1 of the Supplemental Material [32]) were excited by picosecond, 4.75 MHz laser pulses at the wavelength of either 266 or 400 nm. The 400 nm laser is associated with a photon energy of $\sim 1.64\, E_g$, so that it can serve as a reference excitation source without triggering the CM effect. With $\langle N \rangle$ representing the average number of photons absorbed per NC per pulse, the pump fluence of the 400 nm laser was set at either $\langle N \rangle = \sim 0.1$ or ~0.5,

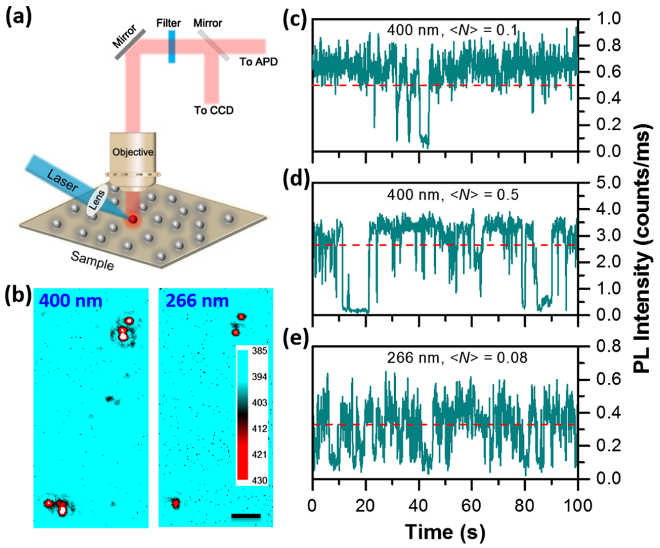


FIG. 2. (a) Experimental setup for the UV-excited single-NC PL measurement. (b) PL images of the same sample region excited at 400 with $\langle N \rangle = \sim 0.1$ (left) and 266 nm with $\langle N \rangle = \sim 0.08$ (right), respectively. The color map used for the two PL images is shown in the inset where the numbers on the right are CCD counts acquired within an integration time of 1 s. The scale bar represents 3 $\mu$m. PL time trajectories of the same single NC excited at 400 with $\langle N \rangle = \sim 0.1$ (c), 400 with $\langle N \rangle = \sim 0.5$ (d), and 266 nm with $\langle N \rangle = \sim 0.08$ (e), respectively. The red dashed lines mark the intensity thresholds above which the fluorescent photons are considered to be from the on levels. The binning time for plotting the PL time trajectories is 100 ms.

while that of the 266 nm laser was set at $\langle N \rangle = \sim 0.08$ (see Supplemental Material [32] for the estimation of $\langle N \rangle$). In Fig. 2(b), we present two PL images of the same sample region excited at 400 ($\langle N \rangle = \sim 0.1$) and 266 nm ($\langle N \rangle = \sim 0.08$), respectively. At both laser wavelengths, the background fluorescence was significantly suppressed, so that we could isolate the same single NC to obtain its PL time trajectories and on-level PL decay curves from the time-tagged, time-resolved (TTTR) measurements.

In Figs. 2(c)–2(e) we plot the PL time trajectories of a representative CdSe NC excited at 400 ($\langle N \rangle = \sim 0.1$), 400 ($\langle N \rangle = \sim 0.5$), and 266 nm ($\langle N \rangle = \sim 0.08$), respectively. Very similar PL time trajectories were obtained from all of the ~50 single CdSe NCs studied in our experiment (see Figs. S2–S4 of the Supplemental Material [32]). When excited at 400 nm with $\langle N \rangle = \sim 0.1$ [Fig. 2(c)], the single CdSe NC was occupied mainly by single excitons and its PL intensity stayed more likely at the on level than at the off level. When excited at 400 nm with $\langle N \rangle = \sim 0.5$ [Fig. 2(d)], the probability for the generation of two excitons in a single NC would be increased and more frequent switching of its PL intensity from the on to the off levels was observed. This kind of photocharging effect has been widely discussed in previous PL blinking studies of single CdSe NCs [19–21,25,26] and can be well explained by the scenario shown in Fig. 1(d) where the electron in a single exciton is

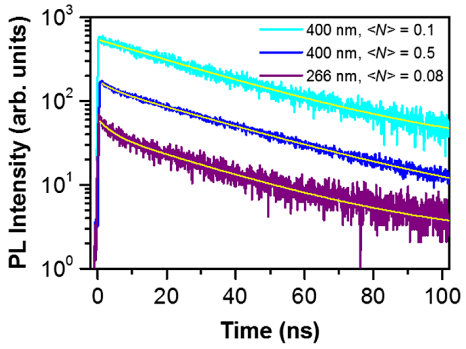


FIG. 3. On-level PL decay curves of the same single NC excited at 400 with $\langle N\rangle = \sim 0.1$ (top), 400 with $\langle N\rangle = \sim 0.5$ (middle), and 266 nm with $\langle N\rangle = \sim 0.08$ (bottom), respectively. The PL decay curve measured at 400 nm with $\langle N\rangle = \sim 0.1$ is fitted by a monoexponential function, while those measured at 400 with $\langle N\rangle = \sim 0.5$ and 266 nm with $\langle N\rangle = \sim 0.08$ are each fitted by a biexponential function. The three PL decay curves are offset to each other for clarity. See Fig. S5 of the Supplemental Material [32] for the same PL decay curves plotted at a larger time window.

ejected out of the NC after receiving the biexciton recombination energy. When the excitation wavelength was changed to 266 nm at $\langle N\rangle = \sim 0.08$ [Fig. 2(e)], fast switching of the PL intensity from the on to the off levels was dramatically enhanced, which should be a direct evidence for the capture of hot electrons into external traps as schematically shown in Fig. 1(e). This is consistent with what was reported previously in single CdSe NCs that laser excitation above the NC band gap would yield fewer long on levels than the excitation on the band gap [23,24].

As shown in Fig. 3 with the 400 nm excitation ($\langle N\rangle = \sim 0.1$), the PL decay curve extracted from the on-level photons of the PL time trajectory in Fig. 2(c) can be well fitted with a monoexponential lifetime of ~33.5 ns, which should arise from the radiative decay of single excitons. Still in Fig. 3 for the 400 nm excitation of the same single NC at $\langle N\rangle = \sim 0.5$, the PL decay curve extracted from the on-level photons of the PL time trajectory in Fig. 2(d) can only be fitted well with a biexponential function of $A_1 e^{-t/\tau_1} + A_2 e^{-t/\tau_2}$, with $A_1$ ($A_2$) and $\tau_1$ ($\tau_2$) being the amplitude and the value of the slow (fast) lifetime component, respectively. The slow lifetime $\tau_1$ of ~35.6 ns can still be attributed to the radiative recombination of single excitons, while the fast lifetime $\tau_2$ of ~3.9 ns, whose amplitude contribution $A_2/(A_1 + A_2)$ is ~13.7%, should be mainly determined by nonradiative Auger decay of biexcitons generated in a single NC after simultaneous absorption of two excitation photons [6,7]. Finally, for the same single NC excited at 266 nm with $\langle N\rangle = \sim 0.08$, the PL decay curve extracted from the on-level photons of the PL time trajectory in Fig. 2(e) is also shown in Fig. 3, which can only be fitted well by a biexponential function with a slow lifetime $\tau_1$ of ~31.7 ns from radiative decay of single excitons. Meanwhile, the fast lifetime $\tau_2$ of ~3.7 ns is almost equal to that measured at 400 nm with $\langle N\rangle = \sim 0.5$, and its amplitude contribution $A_2/(A_1 + A_2)$ is at a higher value of ~30.0%, although the average number of photons absorbed per pulse for this NC has been significantly decreased.

In Figs. S6–S8 of the Supplemental Material [32], the on-level PL decay curves measured at 400 ($\langle N\rangle = \sim 0.1$), 400 ($\langle N\rangle = \sim 0.5$), and 266 nm ($\langle N\rangle = \sim 0.08$) are presented for another three CdSe NCs and very similar trends to those shown in Fig. 3 can be observed. The on-level PL decay curve measured for each of the ~50 single NCs excited at 266 nm with $\langle N\rangle = \sim 0.08$ can be fitted well only by a biexponential function. For each of these ~50 single NCs, we have plotted its biexciton lifetime extracted from the on-level PL decay curve measured at 400 nm with $\langle N\rangle = \sim 0.5$ as a function of its fast lifetime extracted from the on-level PL decay curve measured at 266 nm with $\langle N\rangle = \sim 0.08$. The resulting data points shown in Fig. 4(a) are distributed almost evenly around the diagonal line, thus providing a strong proof for the assignment of the fast lifetime measured at 266 nm with $\langle N\rangle = \sim 0.08$ to nonradiative Auger decay of CM-induced biexcitons. To make sure that the single NCs were not damaged to introduce any unwanted PL decay dynamics during the sequential excitations at 400 nm with $\langle N\rangle = \sim 0.1$, 400 nm with $\langle N\rangle = \sim 0.5$ and 266 nm with $\langle N\rangle = \sim 0.08$, we normally switched back to the 400 nm excitation with $\langle N\rangle = \sim 0.1$ and the same monoexponential lifetime component could be recovered (see Fig. S9 in the Supplemental Material [32]).

When two electrons and two holes are dwelling in a single NC at room temperature, they can be treated as free carriers so that the ratio between single-exciton and biexciton radiative lifetimes is expected to be four [12,34–36]. Then the CM efficiency for biexciton generation can be calculated from $A_2(\tau_1 - \tau_2)/[A_1(3\tau_1 - 4\tau_2) - A_2\tau_2]$ (see the Supplemental Material [32] for the CM efficiency calculation), which is ~15.9% for the PL decay curve shown in Fig. 3 with the 266 nm excitation at $\langle N\rangle = \sim 0.08$. In Fig. 4(b), we present a histogram for the CM efficiencies calculated from similar PL decay curves measured for ~50 single CdSe NCs in our experiment. The distribution of this CM efficiency, with an average value of ~20.2%, roughly reflects the $E_g$ variance from NC to NC due to the size and/or shape heterogeneities [33]. With the excitation wavelength of 266 nm at $\sim 2.46\,E_g$, the CM efficiency of ~20.2% extracted here from single CdSe NCs is comparable to that of ~17.1% measured for similar CdSe NCs with the ensemble energy transfer approach [37].

In addition to the energy-conservation-based limit of $2\,E_g$, an extra energy is normally needed by the optical selection rules in order to trigger the CM effect in semiconductor CdSe NCs [38,39]. With the laser pump fluences at $\langle N\rangle = \sim 0.08$, we also tuned the excitation wavelengths to 283 and 295 nm, corresponding to the photon energies of $\sim 2.31 E_g$ and $\sim 2.22\,E_g$, respectively. With the 283 nm

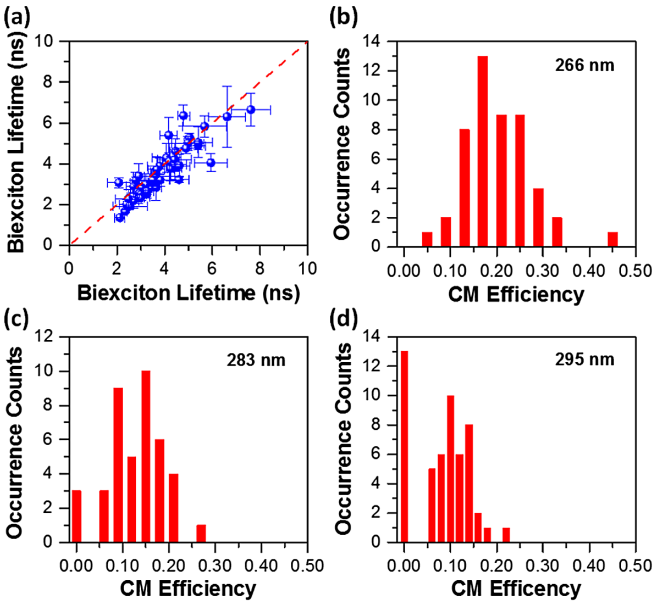


FIG. 4. (a) For the same single NC, the biexciton lifetime extracted from the PL decay curve measured at 400 nm with $\langle N\rangle = \sim 0.5$ is plotted as a function of the biexciton lifetime extracted from the PL decay curve measured at 266 nm with $\langle N\rangle = \sim 0.08$. Distribution histograms for the CM efficiencies of biexciton generation calculated from the on-level PL decay curves of ~50 single NCs excited at 266 nm with $\langle N\rangle = \sim 0.08$ (b), ~40 single NCs excited at 283 nm with $\langle N\rangle = \sim 0.08$ (c), and ~50 single NCs excited at 295 nm with $\langle N\rangle = \sim 0.08$ (d).

excitation, the on-level PL decay curves for three of the ~40 single CdSe NCs studied in our experiment could be accurately fitted by a monoexponential function, while those for all the other NCs still by a biexponential one. In Fig. 4(c), we plot a histogram for the CM efficiencies calculated from the PL decay curves of the ~40 single CdSe NCs excited at 283 nm and an average value of ~13.4% can be obtained. With the 295 nm excitation, the on-level PL decay curves for 13 of the ~50 single CdSe NCs studied in our experiment could be accurately fitted by a monoexponential function, and an average value of ~8.4% can be calculated from the CM efficiency histogram plotted in Fig. 4(d) for these ~50 single CdSe NCs. We can conclude here that the extra energy needed to trigger the CM effect should be even lower than $\sim 0.22\,E_g$, although it is impractical for us to increase the excitation wavelength further due to the lack of enough laser power.

To summarize, we have demonstrated at the single-NC level that the CM efficiency of biexciton generation decreases from ~20.2%, ~13.4%, to ~8.4% when the UV excitation wavelength was sequentially increased from 266 ($\sim 2.46\,E_g$), 283 ($\sim 2.31\,E_g$), to 295 nm ($\sim 2.22\,E_g$). Equipped with the UV-excited single-NC PL technique, we are optimistic that several challenging works could be done in the near future to gain more physical insights into the CM effect of semiconductor NCs. First, no obvious correlation between the CM efficiency and the biexciton lifetime of a single NC was detected in our experiment (see Fig. S14 in the Supplemental Material [32]), implying that the NC-to-NC variation of CM efficiency shown in Figs. 4(b)–4(d) might originate from the difference in energy gap instead of Auger interaction. It would be instructive to perform the single-NC CM measurement at a certain cryogenic temperature so that the single-NC PL linewidth becomes narrow enough to reflect its real energy gap and at the same time the Auger (also the CM) effect is not significantly suppressed [33]. Second, it would be a complementary work to excite the same single NC with a fixed energy gap to compare the PL time trajectories and to depict how the CM efficiency evolves at different UV wavelengths. Third, it would be very helpful if the PL collection efficiency of the optical setup can be greatly improved not only to yield a better signal-to-noise ratio but also to allow the second-order photon-correlation measurement to further confirm the existence of CM-induced biexcitons.

This work is supported by the National Basic Research Program of China (No. 2012CB921801), the National Natural Science Foundation of China (No. 11574147, No. 91321105, No. 11274161, and No. 11321063), Jiangsu Provincial Funds for Distinguished Young Scientists (No. BK20130012), and the PAPD of Jiangsu Higher Education Institutions.

*Corresponding author.
wxiaoyong@nju.edu.cn
†brahim.lounis@u-bordeaux.fr,
‡mxiao@uark.edu

[1] V. I. Klimov, A. A. Mikhailovsky, S. Xu, A. Malko, J. A. Hollingsworth, C. A. Leatherdale, H.-J. Eisler, and M. G. Bawendi, Science **290**, 314 (2000).
[2] V. Sukhovatkin, S. Hinds, L. Brzozowski, and E. H. Sargent, Science **324**, 1542 (2009).
[3] J. B. Sambur, T. Novet, and B. A. Parkinson, Science **330**, 63 (2010).
[4] O. E. Semonin, J. M. Luther, S. Choi, H.-Y. Chen, J. Gao, A. J. Nozik, and M. C. Beard, Science **334**, 1530 (2011).
[5] W. K. Bae, Y.-S. Park, J. Lim, D. Lee, L. A. Padilha, H. McDaniel, I. Robel, C. Lee, J. M. Pietryga, and V. I. Klimov, Nat. Commun. **4**, 2661 (2013).
[6] B. Fisher, J. M. Caruge, D. Zehnder, and M. Bawendi, Phys. Rev. Lett. **94**, 087403 (2005).
[7] V. I. Klimov, A. A. Mikhailovsky, D. W. McBranch, C. A. Leatherdale, and M. G. Bawendi, Science **287**, 1011 (2000).
[8] R. D. Schaller and V. I. Klimov, Phys. Rev. Lett. **92**, 186601 (2004).
[9] R. J. Ellingson, M. C. Beard, J. C. Johnson, P. Yu, O. I. Micic, A. J. Nozik, A. Shabaev, and A. L. Efros, Nano Lett. **5**, 865 (2005).
[10] M. C. Beard, K. P. Knutsen, P. Yu, J. M. Luther, Q. Song, W. K. Metzger, R. J. Ellingson, and A. J. Nozik, Nano Lett. **7**, 2506 (2007).

[11] G. Nair and M. G. Bawendi, Phys. Rev. B **76**, 081304 (2007).
[12] J. A. McGuire, J. Joo, J. M. Pietryga, R. D. Schaller, and V. I. Klimov, Acc. Chem. Res. **41**, 1810 (2008).
[13] M. Ben-Lulu, D. Mocatta, U. Banin, and S. Ruhman, Nano Lett. **8**, 1207 (2008).
[14] M. T. Trinh, A. J. Houtepen, J. M. Schins, T. Hanrath, J. Piris, W. Knulst, A. P. L. M. Goossens, and L. D. A. Siebbeles, Nano Lett. **8**, 1713 (2008).
[15] J. J. H. Pijpers, R. Ulbricht, K. J. Tielrooij, A. Osherov, Y. Golan, C. Delerue, G. Allan, and M. Bonn, Nat. Phys. **5**, 811 (2009).
[16] G. Nair, L.-Y. Chang, S. M. Greyer, and M. G. Bawendi, Nano Lett. **11**, 2145 (2011).
[17] M. Califano, ACS Nano **3**, 2706 (2009).
[18] P. Tyagi and P. Kambhampati, J. Chem. Phys. **134**, 094706 (2011).
[19] K. T. Shimizu, R. G. Neuhauser, C. A. Leatherdale, S. A. Empedocles, W. K. Woo, and M. G. Bawendi, Phys. Rev. B **63**, 205316 (2001).
[20] C. Galland, Y. Ghosh, A. Steinbrück, J. A. Hollingsworth, H. Htoon, and V. I. Klimov, Nat. Commun. **3**, 908 (2012).
[21] N. Yoshikawa, H. Hirori, H. Watanabe, T. Aoki, T. Ihara, R. Kusuda, C. Wolpert, T. K. Fujiwara, A. Kusumi, Y. Kanemitsu, and K. Tanaka, Phys. Rev. B **88**, 155440 (2013).
[22] L. A. Padilha, I. Robel, D. C. Lee, P. Nagpal, J. M. Pietryga, and V. I. Klimov, ACS Nano **5**, 5045 (2011).
[23] K. L. Knappenberger, Jr., D. B. Wong, Y. E. Romanyuk, and S. R. Leone, Nano Lett. **7**, 3869 (2007).
[24] K. L. Knappenberger, Jr., D. B. Wong, W. Xu, A. M. Schwartzberg, A. Wolcott, J. Z. Zhang, and S. R. Leone, ACS Nano **2**, 2143 (2008).
[25] M. Nirmal, B. O. Dabbousi, M. G. Bawendi, J. J. Macklin, J. K. Trautman, T. D. Harris, and L. E. Brus, Nature (London) **383**, 802 (1996).
[26] A. L. Efros and M. Rosen, Phys. Rev. Lett. **78**, 1110 (1997).
[27] S. Rosen, O. Schwartz, and D. Oron, Phys. Rev. Lett. **104**, 157404 (2010).
[28] H. Htoon, J. A. Hollingsworth, R. Dickerson, and V. I. Klimov, Phys. Rev. Lett. **91**, 227401 (2003).
[29] P. Michler, A. Imamoğlu, M. D. Mason, P. J. Carson, G. F. Strouse, and S. K. Buratto, Nature (London) **406**, 968 (2000).
[30] J. A. McGuire, M. Sykora, J. Joo, J. M. Pietryga, and V. I. Klimov, Nano Lett. **10**, 2049 (2010).
[31] A. G. Midgett, H. W. Hillhouse, B. K. Hughes, A. J. Nozik, and M. C. Beard, J. Phys. Chem. C **114**, 17486 (2010).
[32] See Supplemental Material at http://link.aps.org/supplemental/10.1103/PhysRevLett.116.106404 for the experimental details; estimation of the number of excitons created in a single NC; exclusion of charged-exciton contribution to the CM signal; theoretical model for the CM efficiency calculation; solution absorption and emission spectra of ensemble NCs; PL time trajectories of single NCs; on-level PL decay curves of single NCs; distribution graphs for single-NC PL intensities; exciton number dependence of single-NC on-level PL intensities; single-NC CM efficiency plotted as a function of the biexciton lifetime.
[33] Y. Louyer, L. Biadala, J.-B. Trebbia, M. J. Fernée, Ph. Tamarat, and B. Lounis, Nano Lett. **11**, 4370 (2011).
[34] V. I. Klimov, J. A. McGuire, R. D. Schaller, and V. I. Rupasov, Phys. Rev. B **77**, 195324 (2008).
[35] A. F. Cihan, P. L. H. Martinez, Y. Kelestemur, E. Mutlugun, and H. V. Demir, ACS Nano **7**, 4799 (2013).
[36] J. Zhao, O. Chen, D. B. Strasfeld, and M. G. Bawendi, Nano Lett. **12**, 4477 (2012).
[37] J. Xiao, Y. Wang, Z. Hua, X. Wang, C. Zhang, and M. Xiao, Nat. Commun. **3**, 1170 (2012).
[38] R. D. Schaller, V. M. Agranovich, and V. I. Klimov, Nat. Phys. **1**, 189 (2005).
[39] R. D. Schaller, M. A. Petruska, and V. I. Klimov, Appl. Phys. Lett. **87**, 253102 (2005).